STEM CELLS®

TISSUE-SPECIFIC STEM CELLS

Nitric Oxide-Induced Murine Hematopoietic Stem Cell Fate Involves Multiple Signaling Proteins, Gene Expression, and Redox Modulation

AMANDA NOGUEIRA-PEDRO,[a] CAROLINA C. DIAS,[b] HELENA REGINA, C. SEGRETO,[c] PRISCILLA C. ADDIOS,[c] LISANDRO. LUNGATO,[d] VANIA D'ALMEIDA,[d] CARLOS C. BARROS,[e] ELISA M. S. HIGA,[f] MARCUS V. BURI,[b] ALICE T. FERREIRA,[a] EDGAR JULIAN PAREDES-GAMERO[b]

Key Words. Hematopoietic stem cells • Bone marrow • Differentiation • Proliferation

[a]Departamento de Biofísica, [b]Departamento de Bioquímica, [c]Departamento de Oncologia Clínica e Experimental, [d]Departamento de Psicobiologia, and [f]Departamento de Nefrologia, Universidade Federal de São Paulo, São Paulo, Brasil; [e]Faculdade de Nutrição, Universidade Federal de Pelotas, Rio Grande do Sul, Brasil

Correspondence: Edgar Julian Paredes-Gamero, Ph.D., Universidade Federal de São Paulo, Rua Pedro de Toledo, 669-9 andar, Vila Clementino, São Paulo, SP 04039-032, Brasil. Telephone: 55-11-5576-4868; Fax: 55-11-5571–5780; e-mail: edgar.gamero@unifesp.br

Received March 28, 2014; accepted for publication May 30, 2014; first published online in STEM CELLS *EXPRESS* June 26, 2014.

© AlphaMed Press
1066-5099/2014/$30.00/0

http://dx.doi.org/10.1002/stem.1773

ABSTRACT

There are a growing number of reports showing the influence of redox modulation in cellular signaling. Although the regulation of hematopoiesis by reactive oxygen species (ROS) and reactive nitrogen species (RNS) has been described, their direct participation in the differentiation of hematopoietic stem cells (HSCs) remains unclear. In this work, the direct role of nitric oxide ($NO^{\bullet}$), a RNS, in the modulation of hematopoiesis was investigated using two sources of $NO^{\bullet}$, one produced by endothelial cells stimulated with carbachol in vitro and another using the $NO^{\bullet}$-donor S-nitroso-*N*-acetyl-D,L-penicillamine (SNAP) in vivo. Two main $NO^{\bullet}$ effects were observed: proliferation of HSCs—especially of the short-term HSCs—and its commitment and terminal differentiation to the myeloid lineage. $NO^{\bullet}$-induced proliferation was characterized by the increase in the number of cycling HSCs and hematopoietic progenitor cells positive to BrdU and Ki-67, upregulation of Notch-1, Cx43, PECAM-1, CaR, ERK1/2, Akt, p38, PKC, and c-Myc. $NO^{\bullet}$-induced HSCs differentiation was characterized by the increase in granulocytic-macrophage progenitors, granulocyte–macrophage colony forming units, mature myeloid cells, upregulation of *PU.1*, and *C/EBPα* genes concomitantly to the downregulation of *GATA-3* and *Ikz-3* genes, activation of Stat5 and downregulation of the other analyzed proteins mentioned above. Also, redox status modulation differed between proliferation and differentiation responses, which is likely associated with the transition of the proliferative to differentiation status. Our findings provide evidence of the role of $NO^{\bullet}$ in inducing HSCs proliferation and myeloid differentiation involving multiple signaling. STEM CELLS *2014;32:2949–2960*

INTRODUCTION

Recently, a new field of study about the biological functions of reactive oxygen (ROS) and nitrogen (RNS) species has emerged. These molecules are recognized as second messengers that impart a wide range of effects on the body related to aging, pathologies, and the regulation of many biological systems such as the hematopoietic system [1, 2].

Among the RNS, nitric oxide ($NO^{\bullet}$) that is physiologically produced by different cell types, such as endothelial cells, has been implicated in various biological responses [3]. $NO^{\bullet}$ is a short-lived free radical of structural simplicity but complex chemistry, playing critical roles in autocrine and paracrine signaling for the regulation of neuronal, immune, and cardiovascular systems [4]. $NO^{\bullet}$ is endogenously produced by a family of $NO^{\bullet}$ synthases located on mammalian cells plasma membrane, through L-arginine catalysis [4]. Aside from endogenous $NO^{\bullet}$, several classes of exogenous $NO^{\bullet}$ carriers have been developed. These donors are capable of sustained $NO^{\bullet}$ production in a predictable estimated dose, such a feature that has been explored as a useful tool in studying the biological properties of $NO^{\bullet}$ in cells and in in vivo models [6].

According to the hierarchical model of hematopoiesis, all hematopoietic cells are derived from a rare population of hematopoietic stem cells (HSCs) [7]. HSCs reside within specific microenvironments, and for years, these have been mainly referred to as the endosteal and the perivascular niches [8]. However, different niche models continue to emerge [8, 9]. The maintenance of quiescent HSCs in the endosteal niche is supported by cell–cell interactions with stromal cells and/or interaction with matrix elements, which also involve signaling pathways of different molecules such as Notch-1, Jagged1, calcium-sensitive receptor (CaR), Connexin-43 (Cx43), *N*-cadherin, and so on [10, 11]. The release of HSCs from the endosteum to the vascular

 ©AlphaMed Press 2014

niche is mainly associated with their myeloid commitment [12, 13]. The differentiation process is governed by a complex molecular signaling, in which probably the most well established regulators are the cytokines [14]. However, other molecules such ATP, vitamins, and also ROS and RNS, possess the potential ability to modulate hematopoiesis [15–17].

Once $NO^{\bullet}$ can be produced by both endothelial and bone marrow cells in the vascular niche [18, 19], in this work, the role of $NO^{\bullet}$ in the modulation of hematopoietic cell fate was investigated. To address this issue, the direct effect of $NO^{\bullet}$ from endogenous and exogenous sources on hematopoietic cell proliferation and differentiation was evaluated.

Materials and Methods

Animals

The 3-month-old male C57BL/6 mice used in this study were supplied by INFAR/UNIFESP Animal Facility. Green fluorescent protein (GFP) mice (C57BL/6-Tg(act-EGFP)C14-Y01-FM131Osb) were purchased from Centro de Desenvolvimento de Modelos Experimentais para Medicina e Biologia – CEDEME/Universidade Federal de São Paulo. All experiments were approved by the Animal Care Ethics Committee of Universidade Federal de Sâo Paulo (1890/09). Mice were euthanized by cerebral concussion and the bone marrow was extracted from femoral cavity.

Endothelial and Hematopoietic Cell Culture Using a Transwell System

The endothelial cell line of rabbit aorta (kindly provided by Dr. Helena B. Nader), were maintained in HAM's F-12 (Cultilab, Sao Paulo, Brazil, www.cultilab.com.br) medium, supplemented with 10% fetal bovine serum, in a CO_2 humidified incubator at 37°C. A transwell insert of 0.45 micrometers (Merck-Millipore, Darmstadt, Germany, www.emdmillipore.com) was added in each well, in which 5×10^6 bone marrow cells in Dulbecco's modified Iscove's medium (Life Technologies, Carlsbad, CA, www.lifetechnologies.com) were placed. To induce $NO^{\bullet}$ production, endothelial cells were stimulated with carbachol (CCh, Sigma-Aldrich, St. Louis, MO, www.sigmaaldrich.com) [20], which diffused through the medium reaching the hematopoietic cells in suspension in the transwell insert. As control, hematopoietic cells were stimulated with CCh in the absence of endothelial cells monolayer. The diagrammatic scheme of the established culture system is shown in Supporting Information Figure 1.

Long-Term Bone Marrow Culture

Long-term bone marrow culture (LTBMC) was established as described previously [21]. In addition, c-Kit$^+$ cells from bone marrow isolated using EasySep magnetic beads (Stem Cell Technologies, Vancouver, Canada, www.sigmaaldrich.com) following the manufacturer's instructions, were stimulated with CCh in the transwell system and placed above LTBMC stroma, where they remained for seven days. Next, nonadherent cells were collected and immunophenotyped by flow cytometry (FACSCalibur, Becton Dickinson, Franklin Lakes, NJ, www.bdbiosciences.com).

In Vivo Treatment with SNAP

Mice were intraperitoneally treated with 1–3 doses (0.1 mg/kg) of S-nitroso-*N*-acetyl-D,L-penicillamine (SNAP, Life Technologies), an $NO^{\bullet}$ donor. Control animals received only the vehicle (0.008% dimethyl sulphoxide in PBS). Twenty-four hours after the last dose, the mice were euthanized for bone marrow extraction.

Immunolabeling

To identify the different bone marrow cell populations, 1×10^6 cells were labeled with antibody cocktails (all purchased from Becton Dickinson), as detailed in Supporting Information Table 1. A total of 300 000 events for primitive populations and 50 000 events for mature populations were acquired by flow cytometry. Cell Quest software version 3.4 (Becton Dickinson), and FlowJo version 7.6.4 (Tree Star) softwares were used for data acquisition and data analysis respectively. The flow cytometry strategy used is shown in Supporting Information Figure 2. For Ki-67, cell cycle, BrdU, and protein expression assays anti-CD90-FITC was not used.

BrdU Assay

Control and SNAP-treated mice received a dose of 1 mg of 5-bromo-2′-deoxyuridine (BrdU, Sigma-Aldrich) concomitant to the SNAP treatment. BrdU labeling on hematopoietic cells was performed as described previously [22]. Data acquisition was performed by flow cytometry.

Intracellular Proteins and Ki-67 Labeling

Approximately 2×10^6 bone marrow cells were fixed with 2% paraformaldehyde for 20 minutes, washed with glycine 0.1 M, and permeabilized with 0.001% Triton X-100 for 20 minutes. Then the cells were labeled with 3 μl Ki-67-FITC antibody (Becton Dickinson). To label intracellular proteins, cells were incubated for 2 hours with the following antibodies: p-ERK1/2 (Thr204-202/Tyr), p-Stat5, p-PKCpan, p–p38 (Thr182-180/Tyr), p-Akt (Thr308), p–c-Myc (Thr58/Ser62), PECAM-1, Cx43, Notch-1, and CaR. The antibodies were purchased from Becton Dickinson, Cell Signaling (Danvers, Massachusetts, www.cellsignal.com), and/or Santa Cruz (Dallas, Texas, www.scbt.com/pt). Anti-rabbit or goat IgG secondary antibodies conjugated with Alexa Fluor 488 (4 mg/ml) were used for at least 40 minutes. In both situations, antibodies for HSC and hematopoietic progenitor (HP) identification by flow cytometry were used. Protein analyses were performed by quantification of the fluorescence geometric mean.

Cell Cycle Analysis

Approximately 2×10^6 bone marrow cells were fixed and permeabilized as described previously, and treated with 4 mg/ml RNase for 45 minutes at 37°C. For DNA labeling, cells were incubated with 1 μM of SYTO 16 (Life Technologies). Finally, the antibody cocktail was used to identify HSC and HP. Data acquisition was performed by flow cytometry.

Histochemical Analysis

H&E labeling was performed as described elsewhere [23]. Photomicrographs of four sorted regions per femur were obtained using a digital camera DS-Fi1 of an inverted microscope (TS-100, Nikon, Tokyo, Japan, www.nikon.com). Visualization was performed using a 10× dry objective lens (numerical aperture: 0.25). Femur section analysis was performed by the conversion of trabecular and long bone cells into black dot plots, which were quantified using Image J software.

CFU Assay

Approximately 2×10^4 bone marrow cells were mixed with 1 ml of methylcellulose-based medium containing recombinant

cytokines and erythropoietin (Methocult M3434, Stem Cell Technologies). The mixture was placed in 35-mm dishes and cultured in a humidified incubator for 7 days. On the end of this period, colonies consisting of more than 50 cells were counted using an inverted microscope at 40× magnification.

RNA Extraction, cDNA Synthesis, and qRT-PCR Array

Total RNA from c-Kit$^+$ cells was extracted using the RNeasy Mini Kit (Qiagen, Hilden, Germany, www.qiagen.com). A 0.2 μg of intact RNA was used for cDNA synthesis. RNA amplification in real-time was performed on the 7500 Sequence Detection System (Applied Biosystems, Carlsbad, California, www.appliedbiosystems.com) using TaqMan system, following the manufacturer's instructions. Standard curves were generated for each primer to check amplification efficiency. The primers used were: *Ikz-3* (Mm01306721_m1*), *GATA-1* (Mm01352636_m1*), *GATA-2* (Mm00492301_m1*), *GATA-3* (Mm00484683_m1*), *Sfpi-1/PU.1* (Mm00488142_m1*), *C/EBPα* (Mm00514283_s1*), and *NF-E2* (Mm00801891_m1*). Gene expression was normalized to the housekeeping *β-actin* gene expression (*GAPDH* was also tested, resulting in no significant differences from β-actin gene expression) and the results were expressed in relative values using the cycle threshold ($2^{-\Delta\Delta Ct}$). The expression levels of the genes of interest were normalized to the control group.

Bone Marrow Reconstitutive Assay

Transgenic C57BL/6 mice expressing green fluorescent protein (GFP$^+$) were used as bone marrow donors. These animals were treated with SNAP for 1 and 3 days. Twenty-four hours after the last dose, bone marrow was collected and 5×10^6 cells of the GFP$^+$ mice were transplanted via retro-orbital sinus [24] into a C57BL/6 wild-type mice, which were whole-body irradiated with a single dose of 6 Gy (dose rate of 0.4 Gy.min^{-1}) [25] in a ^{60}Co therapy apparatus Alcyon II (CGR, Paris, France) previously to transplantation. Two months later, bone marrow cells of the recipient mice were collected for immunophenotyping by flow cytometry.

Cell Viability Assessment

Approximately 1×10^6 cells were incubated with 50 μl of annexin buffer, 3 μl of annexin V-FITC (Becton Dickinson), and 5 μg/ml of 7-aminoactinomycin D (7-AAD) (Life Technologies) for 20 minutes. In some cases, anti-c-Kit-APC was added. After incubation, cells were washed and resuspended in 200 μl of annexin buffer for data acquisition by flow cytometer.

Intracellular ROS Measurement

Approximately 1×10^6 bone marrow cells were incubated with 5 μM of 5-(and-6)-chloromethyl-2′,7′-dichlorodihydrofluorescein diacetate acetyl ester (CM-H$_2$DCFDA) (Life Technologies) and 1 μM of dihydroetidium (DHE) (Sigma-Aldrich) for 40 minutes at 37°C. The c-Kit$^+$ population was recognized using the appropriate antibody and data acquisition was performed by flow cytometry. For ROS quantification by fluorescence microscopy (DM-6000, Leica, Sao Paulo, Brazil), total bone marrow and c-Kit$^+$ cells were labeled with CM-H$_2$DCFDA and DHE and placed into glass bottom plates. Cells were stimulated with 64 μM of SNAP (equivalent to the dose of 0.1 mg/kg administered in vivo), and the fluorescence of both probes was monitored during 30 minutes.

Antioxidant Enzymes Quantification

Total bone marrow and c-Kit$^+$ purified cells were lysed, centrifuged at 300 rpm for 40 minutes at 4°C in phosphate buffer (100 mM, pH 7.0), and the final supernatant was subjected to the enzymatic analysis. Catalase (Cat) and superoxide dismutase (SOD) activities were measured as described by Adamo et al. [26] and Ewing and Janero [27], respectively. Total protein content used for data normalization was measured using a Bradford Protein Assay Kit (Bio-Rad).

Glutathione Assay

Glutathione (GSH) content was quantified in total bone marrow lysate as described previously [3] using high-performance liquid chromatography.

Hemogram and NO$^\bullet$ Dosage

See Supporting Information Methodology.

Statistical analysis

For data analysis of multiple comparisons among groups, analysis of variance and Bonferroni's post hoc test were performed. Values were expressed as mean ± SEM. Differences were considered significant when $p < 0.05$. Prisma 5 software (Graph Pad Inc.) was used for the statistical analysis.

Results

Endogenous NO$^\bullet$ Induces HSCs Commitment to the Myeloid Lineage

To evaluate the NO$^\bullet$ effects, first, in vitro assays were performed. Bone marrow cells were exposed to NO$^\bullet$ produced by endothelial cells that were stimulated with CCh in the transwell system for 4, 8, and 16 hours. The 8 hours time was chosen for the subsequent experiments based on the significant differences observed in HSC and HP populations (data of 4 and 16 hours are shown in Supporting Information Fig. 3). To confirm NO$^\bullet$ production by endothelial cells, the amount of nitrites and nitrates released into the medium after CCh stimulation was measured. A significant increase in NO$^\bullet$ generation was quantified for all CCh concentrations used (Supporting Information Fig. 4A). The control bone marrow cells that were directly stimulated with the same concentrations of CCh but in the absence of endothelial cells are shown in Figure 1A, 1B. However, because no significant alterations among the control groups were observed, a single control was used for the subsequent experiments. NO$^\bullet$ produced by endothelial cells induced a decrease in the percentage of HSCs (Fig. 1A), whereas an increase in common myeloid progenitor and granulocyte/monocyte progenitor (GMP) populations was observed (Fig. 1B). No alterations in both mature myeloid (Mac-1$^+$Gr-1$^+$) and lymphoid cells (CD3$^+$ and B220$^+$CD19$^+$) as well as in their clonogenic capacity were observed after 8 hours of stimulation (Supporting Information Fig. 5A–5C). Because the duration of CCh stimulation in the transwell system was only 8 hours, a LTBMC was established to confirm cells differentiation. For this purpose, c-Kit$^+$ cells were previously stimulated with NO$^\bullet$ from CCh-stimulated endothelial cells in the transwell system, and then were seeded on the preestablished stroma for 7 days. NO$^\bullet$ produced by endothelial cells induced an increase in HP cells in the LTBMC (Fig. 1C). Moreover, 10 and 100 μM of CCh stimulation resulted in a 45% increase in the myeloid population in the LTBMC (Fig. 1D). To verify if the decreased percentage of HSCs occurred through cell death, an annexin/7AA-D assay was conducted. However, NO$^\bullet$

 ©AlphaMed Press 2014

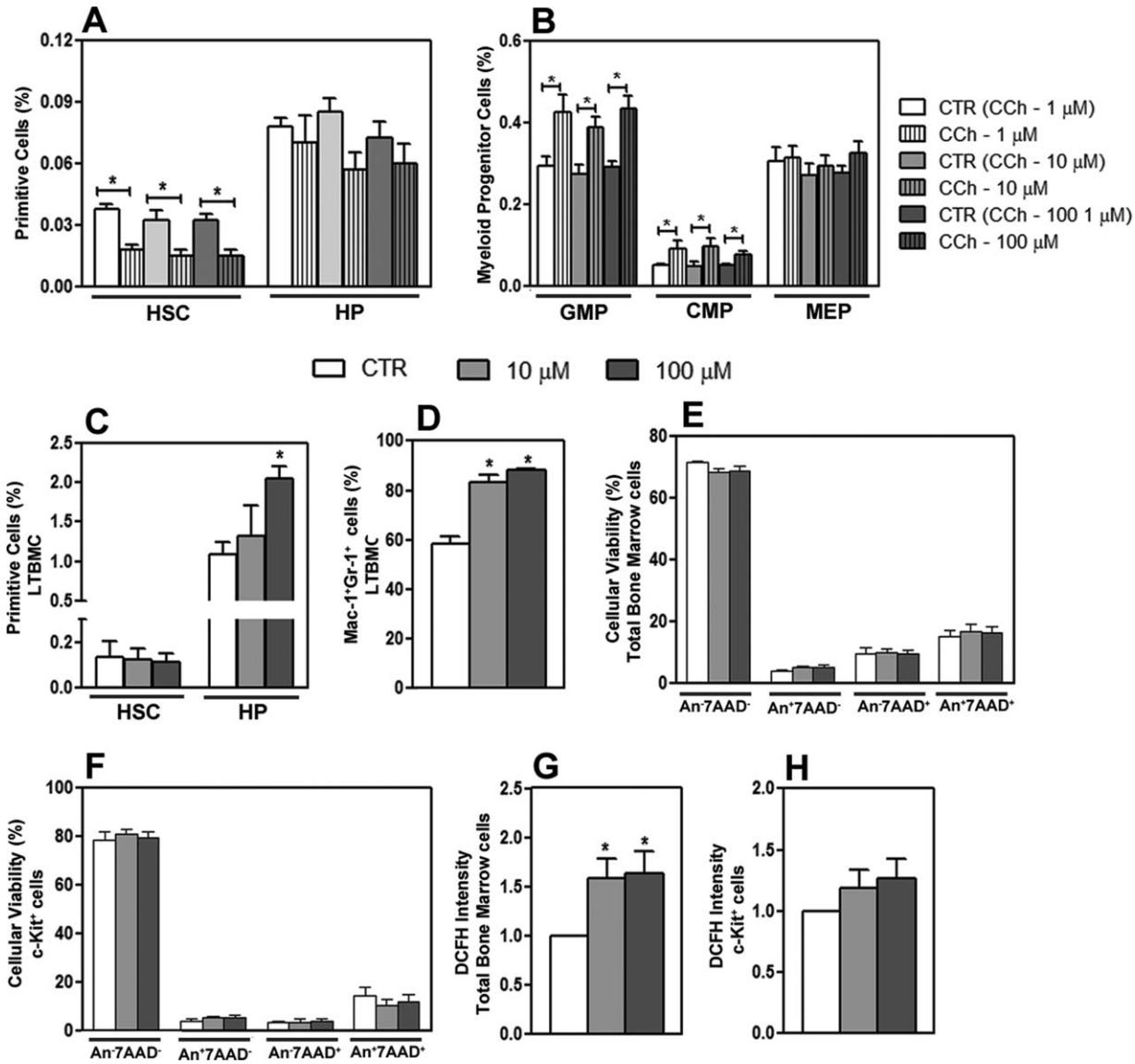

Figure 1. NO• induces differentiation of hematopoietic stem cells (HSCs) into myeloid cells in vitro. **(A, B, E–H):** Coculture of bone marrow cells and endothelial cells for 8 hours in the transwell system. Endothelial cells were stimulated with carbachol (CCh) for NO• production. All data were acquired by flow cytometry. For immunophenotyping, cells were labeled with the respective antibody cocktails and data are showed as a percentage of the total number of bone marrow cells. **(A):** Primitive populations: HSC and hematopoietic progenitor (HP). **(B):** Myeloid progenitors: granulocyte/monocyte progenitor, common myeloid progenitor, and megakaryocyte/erythrocyte progenitor. **(C–D):** Immunophenotyping of bone marrow cells previously stimulated with CCh in the transwell system and cocultivated on stroma of the long-term bone marrow culture system. **(C):** Primitive populations and **(D)** the myeloid mature population of Mac-1^+Gr-1^+ cells. **(E, F):** Viability measured using annexin-V and 7-aminoactinomycin D (7-AAD), showing percentage of viable cells (An^-7-AAD^-), apoptotic cells (An^+7-AAD^-), necrotic cell (An^-7-AAD^+), and necrotic and/or apoptotic cells (An^+7-AAD^+). **(G, H):** Reactive oxygen species levels from cells labeled with 5 μM of CM-H_2DCFDA. Data from CCh-stimulated cells were normalized by DCFH fluorescence geometric mean of the control group. Data are expressed as the mean ± SEM of three independent experiments performed in duplicate. *, $p < .05$ analysis of variance test. Abbreviations: 7-AAD, 7-aminoactinomycin D; CCh, carbachol; CMP, common myeloid progenitor; CTR, control; DCFH, dichlorofluorescin; GMP, granulocyte/monocyte progenitor; HP, hematopoietic progenitors; HSC, hematopoietic stem cells; LTBMC, long-term bone marrow culture; MEP, megakaryocyte/erythrocyte progenitor.

did not induce cell death in both total bone marrow and c-Kit^+ cells (Fig. 1E, 1F), even in the presence of higher ROS levels in CCh stimulated cells in comparison with control cells (Fig. 1G, 1H; Supporting Information Fig. 6), which might have occurred due to antioxidant system imbalance.

NO• Induces the Expansion of HSCs

After the initial in vitro analysis, the in vivo effects of NO• were evaluated by treating mice with SNAP. Treatment effectiveness was confirmed by the elevated nitrite and nitrate levels quantified on the total bone marrow cells lysate after SNAP administration (Supporting Information Fig. 4B).

On the 3rd day of treatment, the increase in percentage of HSCs (Fig. 2A) was an indicative of their proliferative response to NO• stimulation. The proliferative state was confirmed by the BrdU assay, which showed a maximal BrdU incorporation in HSCs on the 1st day of SNAP treatment; HSCs $BrdU^+$ increased 58% on the 1st day of treatment and

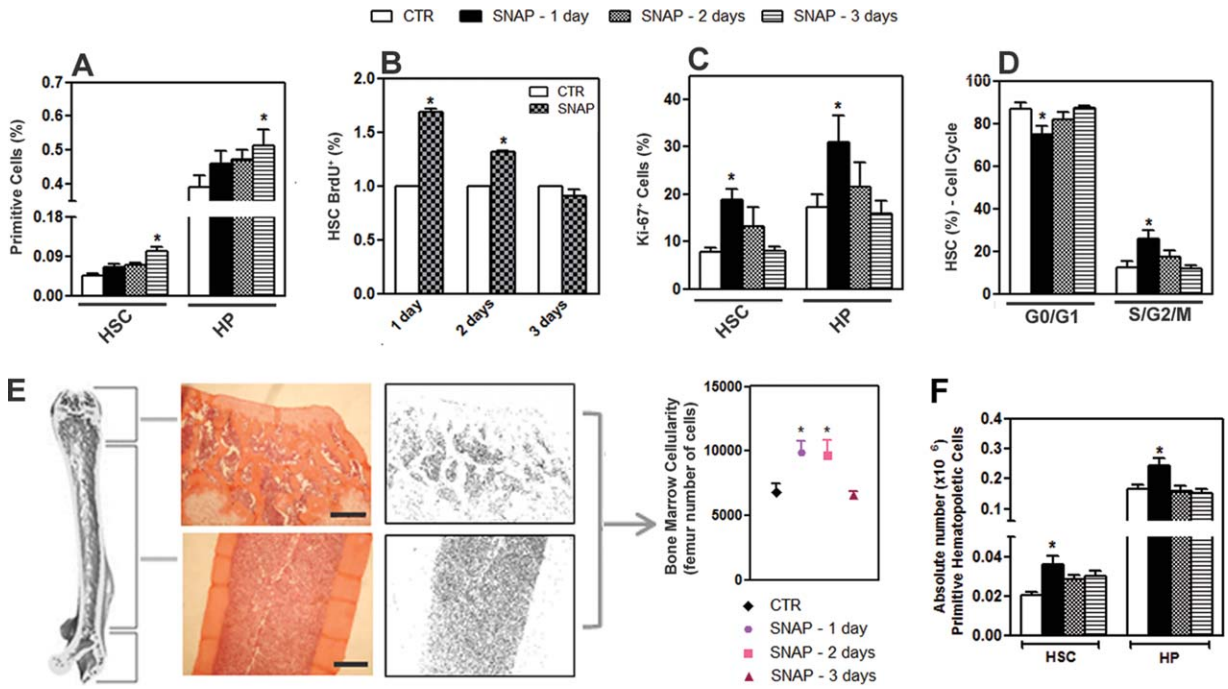

Figure 2. NO• induces hematopoietic stem cells (HSCs) expansion. Mice were treated intraperitoneally with 0.1 mg/kg of S-nitroso-*N*-acetyl-D,L-penicillamine (SNAP) for 1–3 days and then their cells were subjected to various analyses. Cells were labeled with the respective antibody cocktails for HSCs and hematopoietic progenitors (HPs) recognition. **(A–D):** Flow cytometry analysis. **(B–D):** Cells were fixed and permeabilized before antibodies labeling. **(A):** Percentage of HSCs and HPs along the treatment days, $n = 12$. **(B):** Concomitant to SNAP treatment, mice received 1 mg/dose of BrdU, and the percentage of HSCs incorporated with BrdU is shown on the difference of treated mice cells in relation to the control, $n = 4$. **(C):** After SNAP treatment, cells were labeled with Ki-67 to identify the percentage of cycling HSCs and HPs, $n = 6$. **(D):** After permeabilization, cells were treated with 4 mg/ml RNase for 45 minutes at 37°C, before labeling with 1 μM SYTO Green, for evaluation of HSCs and HPs cell cycle phases, $n = 6$. **(E):** Bone marrow cellularity was evaluated in femur slices stained with H&E in trabecular and long bone regions. Photomicrographs were taken using a digital camera attached to an inverted microscope and using a 10× dry objective lens (numerical aperture: 0.25). Cells were quantified using the Image J software. Scale bar = 200 μm, $n = 4$. **(F)** Absolute number of HSCs and HPs, $n = 10$. Data are expressed as the mean ± SEM of independent experiments. *, $p < .05$ analysis of variance test. Abbreviations: CTR, control; HP, hematopoietic progenitor; HSC, hematopoietic stem cells.

progressively decreased during the following days (Fig. 2B). In addition, the expression of Ki-67— a protein exclusively expressed in dividing cells [28]—in HSCs was evaluated, showing the increased HSCs Ki-67$^+$ and HPs Ki-67$^+$ cells by approximately 142% and 79%, respectively (Fig. 2C), which was in agreement with the findings of the BrdU$^+$ assay. Cell cycle analysis showed the exit of HSCs from the G_0/G_1 and their entry into $S/G_2/M$ phase on the 1st day of treatment (Fig. 2D), corroborating the higher proliferative state of HSCs. Representative histograms used as parameter for quantitative analyses described above are shown in Supporting Information Figure 7. Moreover, the proliferative response of HSCs led to bone marrow hyperplasia. Histological analysis of trabecular and long bone areas showed an increase in cell counts on the 1st day of treatment, and a decreasing at the control level on the 3rd day (Fig. 2E). Similarly, absolute counts of HSCs and HPs put in evidence the higher number of primitive cells at the 1st day of SNAP treatment (Fig. 2F).

Myeloid Commitment Is Induced by NO•

Although the expansion of HSCs occurred on the 1st day of treatment, alterations in the differentiated progeny were only observed on the 3rd day. Both GMP and LP populations increased (Fig. 3A, 3B), but only mature myeloid cells (Gr-1$^+$Mac-1$^+$) were augmented (Fig. 3C), whereas erythroid and lymphocyte populations decreased (Fig. 3D). In addition, no significant differences were observed for erythrocyte and leukocyte cell counts from peripheral blood (Supporting Information Fig. 8). To confirm the NO•-induced differentiation, myeloid colony forming unit (CFU) assay was performed. The number of granulocyte–macrophage progenitor (CFU-GM) formed from the 3-days-SNAP-treated cells significantly increased, whereas the number of colonies of granulocytes (G), macrophages (M), megakaryocytes (GEMM), and erythrocytes (burst-forming unit-erythrocytes) did not significantly change (Fig. 3E), corroborating the increased number of granulocytes/macrophage progenitor cells under NO• stimulation.

Furthermore, the expression of genes related to lymphopoiesis and myelopoiesis were quantified. qRT-PCR of c-Kit$^+$ purified cells revealed that on the 1st day of SNAP treatment, except for *PU.1* and *NF-E2*, all the other genes were downregulated 0.5-fold (Fig. 3F) by NO•, whereas on the 3rd day, upregulation of genes associated with myeloid differentiation, such as *C/EBP-α* and *PU.1*, was observed (Fig. 3Fv, 3Fvii), which was concomitant to the decreased expression of *GATA-3* and *Ikz-3* (Fig. 3Fiii, 3Fiv), both associated with lymphoid differentiation.

In Vivo Capacity of Bone Marrow Long-Term Reconstitution Is Reduced by NO•

To verify the stemness of HSCs that underwent proliferation under NO• stimulation, bone marrow reconstitution assay was

 ©AlphaMed Press 2014

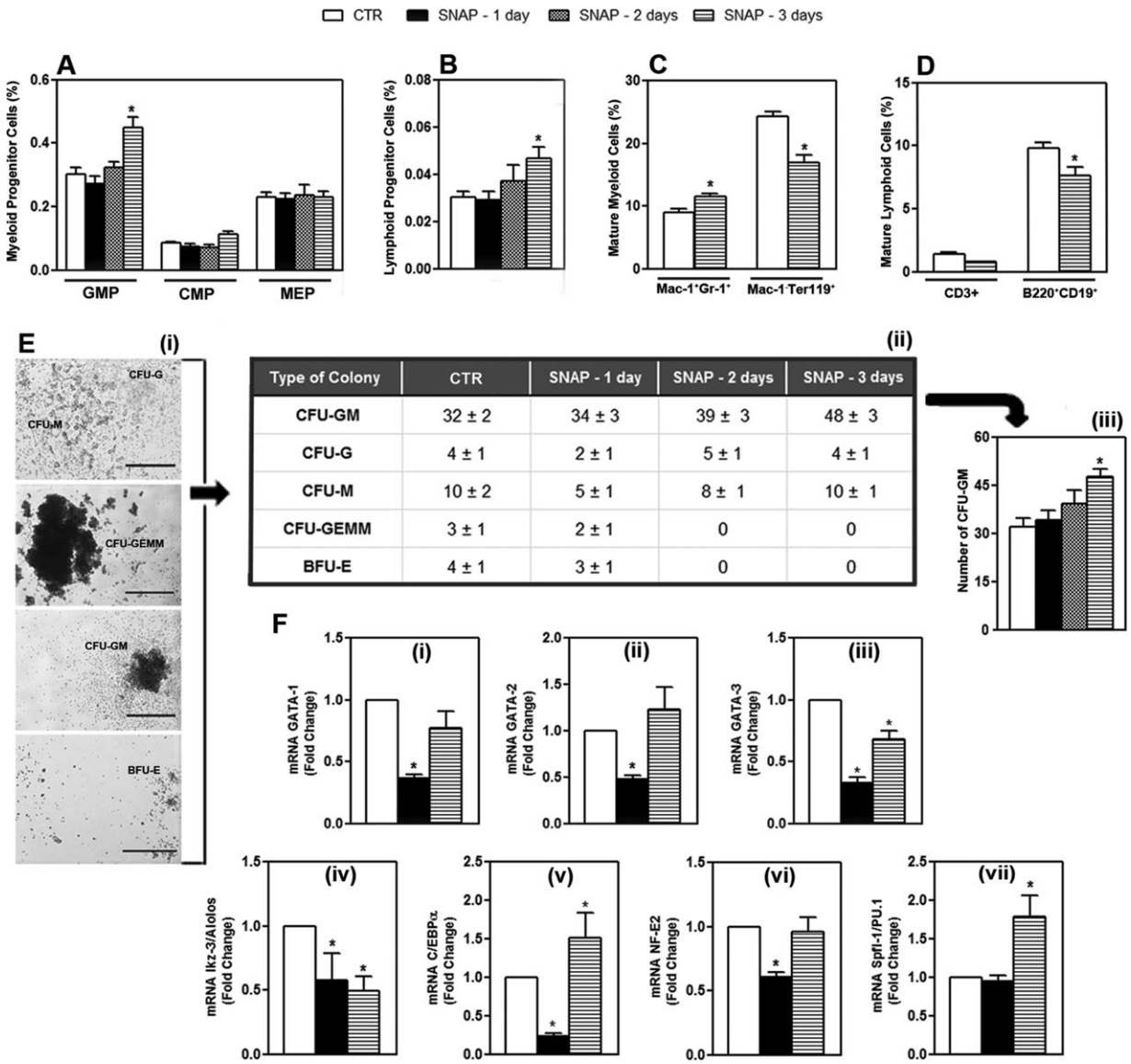

Type of Colony	CTR	SNAP - 1 day	SNAP - 2 days	SNAP - 3 days
CFU-GM	32 ± 2	34 ± 3	39 ± 3	48 ± 3
CFU-G	4 ± 1	2 ± 1	5 ± 1	4 ± 1
CFU-M	10 ± 2	5 ± 1	8 ± 1	10 ± 1
CFU-GEMM	3 ± 1	2 ± 1	0	0
BFU-E	4 ± 1	3 ± 1	0	0

Figure 3. NO•-induced commitment of hematopoietic stem cells (HSCs) into myeloid progeny involves *C/EBPα* and *PU.1* upregulation. Mice were treated intraperitoneally with 0.1 mg/kg of S-nitroso-*N*-acetyl-D,L-penicillamine (SNAP) for 1–3 days and then their cells were subjected to various analyses. Cells were labeled with the respective antibody cocktails for HSCs and hematopoietic progenitors (HPs) recognition by flow cytometry. Data are shown as the percentage of each cell population from the total number of bone marrow cells. **(A):** Myeloid progenitors, $n = 12$. **(B):** Lymphoid progenitors, $n = 12$. Mature **(C)** myeloid cells and **(D)** lymphoid cells, $n = 12$. **(Ei–Eiii):** Colony forming unit (CFU) assay performed in methylcellulose medium using 2×10^4 cells. Colonies consisting of more than 50 cells were counted in a TS-100 inverted microscope after 7 days of culture, using a 4× dry objective lens (numerical aperture: 0.10). **(i):** Representative images of each type of colony were acquired using a digital camera attached to an inverted microscope. Scale bar = 100 μm, $n = 6$. **(ii):** Discriminative table of the total absolute number of colonies counted. **(iii):** Graph showing the increase in the number of granulocyte–macrophage progenitor (GM-CFU) formed by cells from mice treated for 3 days with SNAP. **(F):** qRT-PCR performed with the RNA from c-Kit$^+$ cells using the TaqMan and the 7500 Sequence Detection Systems. Expression of genes associated with the commitment of hematopoietic cells to the myeloid (*PU.1*, *GATA-1*, *GATA-2*, *NF-E2*, and *C/EBPα*) and lymphoid (*GATA-3* and *Ikz-3*) progenies was normalized to the *β-actin* housekeeping gene and is represented in relative values obtained from the cycle threshold ($2^{-\Delta\Delta Ct}$). The expression levels of the genes of interest from the SNAP-treated cells were normalized to the control group, $n = 6$. Data are expressed as the mean ± SEM of independent experiments. *, $p < .05$ analysis of variance test. Abbreviations: BFU, burst-forming unit-erythrocytes; CFU, colony forming unit; CMP, common myeloid progenitor; CTR, control; GEMM, granulocytes, macrophages, megakaryocytes; GM, granulocyte–macrophage; GMP, granulocyte/monocyte progenitor; MEP, megakaryocyte/erythrocyte progenitor; SNAP, S-nitroso-*N*-acetyl-D,L-penicillamine.

performed. Bone marrow cells from GFP$^+$ mice treated for 1 and 3 days with SNAP or not (in this case receiving just the vehicle) were transplanted into sublethally irradiated non-transgenic recipients. After 2 months, the chimerism was evaluated (Fig. 4A). HSC subset from both recipients that received SNAP-treated bone marrow cells showed a lower percentage of HSCs, whereas HPs remained constant (Fig. 4B), which indicates a reduced long-term reconstitutive ability. The formation rate of granulocytes were maintained elevated, being higher in the SNAP-3-days-treated group of recipients (Fig. 4C),

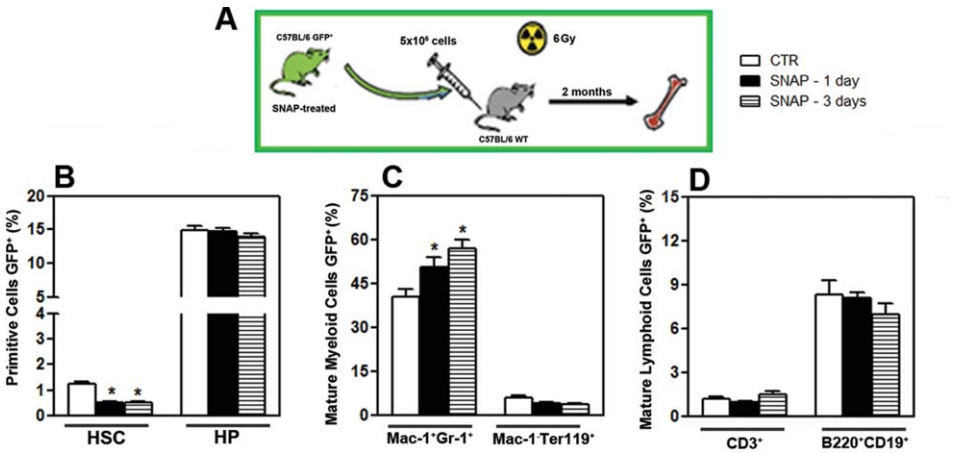

Figure 4. $NO^{\bullet}$ induces a decrease in hematopoietic stem cells (HSCs) long-term repopulation potential. **(A):** Experimental scheme of hematopoietic cells transplantation. Approximately 5×10^6 cells from transgenic mice green fluorescent protein (GFP^+) that were treated intraperitoneally for 1 and 3 days with S-nitroso-*N*-acetyl-D,L-penicillamine (SNAP) (or not) were transplanted via the retro-orbital sinus into sublethally irradiated nontransgenic recipients. After 2 months, bone marrow cells were collected, labeled with antibody cocktails, and immunophenotyped by flow cytometry. **(B):** Percentage of HSCs and hematopoietic progenitors (HPs) GFP^+ engrafted in bone marrow after transplantation. **(C, D):** Mature myeloid and lymphoid cells, respectively, generated from the engrafted HSCs. Data are expressed as the mean ± SEM of three independent experiments, $n = 12$. *, $p < .05$ analysis of variance test. Abbreviations: CTR, control; GFP, green fluorescent protein; HP, hematopoietic progenitor; HSC, hematopoietic stem cells; SNAP, S-nitroso-*N*-acetyl-D,L-penicillamine.

whereas erythroid cells and T and B lymphocytes did no change (Fig. 4D).

Signaling Pathways Involved in $NO^{\bullet}$ Effects

Expression of proteins that participate in proliferation, differentiation, and hematopoietic cell survival [29, 30] were analyzed. On the 1st day of treatment, when the proliferative state of HSCs was augmented, a significant phosphorylation increase in the intracelullar proteins Akt, ERK1/2, p38, PKC, and c-Myc, as well as the upregulation of the membrane proteins Notch-1, Cx43, PECAM, and CaR was observed. Moreover, on the 3rd day of treatment when HSCs were found differentiated, a significant phosphorylation decrease in Akt and c-Myc and downregulation of Cx43 and Notch-1 occurred in relation to control (Fig. 5). However, comparing the phosphorylation and protein expression levels observed in the 3rd in relation to the 1st day, during differentiation and proliferation responses respectively, all proteins—except Stat5 (which was activated) and PECAM-1 (whose levels were not significantly altered)—were significantly downregulated during HSCs differentiation. In addition to the heat map of Figure 5, fluorescence histograms of each protein expression are presented at Supporting Information Figure 9.

Intracellular Antioxidant Mechanisms Contribute to Hematopoietic Cell Fate Under $NO^{\bullet}$ Stimulation

Due to the $NO^{\bullet}$ characteristic of reactivity with a wide range of molecules [3] and because ROS production can be also induced by SNAP [31], cellular viability, and redox status were verified. At the dose of 0.1 mg/kg, SNAP did not confer cytotoxic, either to total bone marrow or to c-Kit^+ cells (Fig. 6A). However, at higher doses of 0.3 and 1 mg/kg, SNAP induced cell death in the primitive population of c-Kit^+ cells (Supporting Information Fig. 10).

Fluorescent probes to measure ROS (especially H_2O_2) and superoxide radicals generation [32] were detected microscopically in a real-time system. The data gathered from total bone marrow cells are presented in Supporting Information Figure 11. SNAP induced the generation of ROS and $O_2^{\bullet -}$ in both total bone marrow and c-Kit^+ cells (Fig. 6B–6Bii). A decrease in DCFH and DHE detection in unstimulated cells might have occurred due to photobleaching in the beginning of data acquisition (Fig. 6Bi, 6Bii; Supporting Information Fig. S11Ai, S11Aii). Moreover, flow cytometry analysis showed an increase in $O_2^{\bullet -}$ levels in both total bone marrow and c-Kit^+ cells, whereas ROS levels did not change in total bone marrow cells and decreased in c-Kit^+ cells on the 3rd day of treatment (Fig. 6C).

Furthermore, antioxidant machinery was evaluated. Cat activity significantly increased on the 1st day of SNAP treatment and progressively decreased in c-Kit^+ cells (Fig. 6D). SOD activity decreased in total bone marrow cells on the 1st day of SNAP treatment (Fig. 6E). Total GSH content increased on the 1st day of SNAP treatment (Fig. 6F). In total bone marrow cells, Cat and SOD activity and GSH content were not significantly affected (Supporting Information Fig. 11C–11E).

Discussion

Several biological functions of $NO^{\bullet}$ have been described other than its remarkable ability to act as a vasodilator [19]. $NO^{\bullet}$ also plays a role as inductor or inhibitor of cellular differentiation and mitogenic activity of different cell types [33].

The mechanistic link between $NO^{\bullet}$ and hematopoiesis may involve modifications of proteins activity, redox regulation, and resetting gene expression patterns in the cell by activating multiple signaling pathways [34]. Some reports describe distinct $NO^{\bullet}$ roles in the modulation of hematopoietic system. During embryogenesis, $NO^{\bullet}$ regulates the establishment of the vascular niche and HSCs production [35]. In adult organism, $NO^{\bullet}$ is necessary for human $CD34^+$ cells differentiation into dendritic cells [36] as well as for HSCs

 ©AlphaMed Press 2014

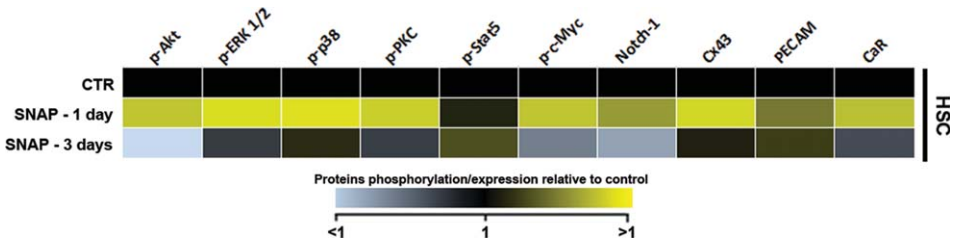

Figure 5. S-nitroso-*N*-acetyl-D,L-penicillamine (SNAP) modulates the activation of signaling pathways and expression of proteins involved in the proliferation and differentiation of hematopoietic stem cells (HSCs). Bone marrow cells from mice-treated intraperitoneally with 0.1 mg/kg of SNAP for 1 and 3 days. Cells were fixed and permeabilized before primary and secondary (Alexa Fluor 488) antibodies labeling (4 μg/ml each) to recognize intracellular proteins and surface molecules, together with the antibodies for HSCs recognition. Data acquisition was performed by flow cytometry. **(A):** Heat map of the geometric mean of fluorescence of each protein, showing the different expression patterns after SNAP treatment in comparison with the control group (black). Increased and decreased phosphorylation/expression ranges from yellow to light blue, respectively.

commitment during megakaryopoiesis [37]. Although $NO^{\bullet}$-induced proliferation has been demonstrated by exogenous $NO^{\bullet}$ stimulation in many cells [38], in the hematopoietic system, previous findings have described the role of endogenous (not exogenous) $NO^{\bullet}$ in the inhibition of HSCs expansion [34]. In this study, two sources of $NO^{\bullet}$ were used: one produced by endothelial cells stimulated with CCh and another donated by SNAP. The in vitro effects of $NO^{\bullet}$ using CCh were verified in short (8 hours) and long-term culture systems (Dexter), whereas the in vivo effects were observed in mice treated with SNAP. Using these models for $NO^{\bullet}$ production in the current study, we have clearly verified the proliferative effect of HSCs and subsequently their differentiation to the myeloid lineage.

The first response produced by $NO^{\bullet}$ was the increased percentage of HSCs and HPs in vivo. The proliferative status of HSC and HP populations were corroborated on the results of BrdU, Ki-67, and cell cycle assays, which showed the high proliferative status of HSCs on the 1st day of treatment, that led to a significant increase in HSC and HP populations on the 3rd day of treatment, probably due to the accumulation of short-term HSCs (ST-HSCs) and other progenitors in the bone marrow. The scenario of increased HSCs $NO^{\bullet}$-induced proliferation on the 1st day of treatment was accompanied by Akt, ERK1/2, p38, PKC, and c-Myc activation, which are proteins related to proliferation and/or differentiation [29, 39–41]. Moreover, the upregulation of the membrane proteins Notch-1, CaR, and PECAM-1 that are mostly involved in the maintenance of HSCs in the endosteal [8, 42] and vascular niches [43], as well as Cx43, which is highly expressed in HSCs and is downregulated during their differentiation [44], were also upregulated. In vitro, the proliferative effect of $NO^{\bullet}$ stimulation was not observed probably because of the short time of culture or even due to the presence of other intrinsic factors such as ATP and cytokines, which possess different roles in HSC modulation [21, 40, 45].

The differentiation process was observed in vitro and in vivo. $NO^{\bullet}$ derived from endothelial cells induced the myeloid commitment, which in turn resulted in HSCs percentage decreasing and GMP population increasing. Similarly, HPs percentage was enhanced in the LTBMC, as well as the myeloid mature cells (Mac-1^{+}Gr-1^{+}). In vivo, the differentiation was observed on the 3rd day of SNAP treatment through the increase in GMP population, CFU-GM and mature myeloid cells, with the activation of genes associated to myelopoiesis such as *PU.1* and *C/EBPα*. Thus, the lower absolute number of HSCs and HPs and the higher percentage of these primitive populations at the 3rd day of treatment in comparison with the 1st day of treatment, can be explained by the prevalence of primitive cells in bone marrow over the differentiated cells due to the release of the mature cells into the circulation. Furthermore, HSCs capability to reconstitute bone marrow for long-periods in lethally irradiated recipient mice, which is an important feature of the undifferentiated state [46], was altered. HSCs from SNAP-treated mice were capable of generating multilineage progeny; however, the number of HSCs was reduced after 2 months, indicating the decreased plasticity of the most primitive HSCs (prevalence of ST-HSCs over long-term HSCs [LT-HSCs]), which was accompanied by the increased generation of myeloid progenitors and mature myeloid cells (predominantly Gr-1^{+}Mac-1^{+}), showing that even after transplantation, myeloid differentiation still occurs in a preferentially fashion in response to $NO^{\bullet}$. An analogous effect was observed with other signaling molecules such as ATP that results in rapid hematopoietic cells proliferation and differentiation [21]. This cellular scenario of differentiation was accompanied by the activation of Stat-5, whereas Cx43 and, Notch-1 expression, as well as Akt and c-Myc phosphorylation decreased (in comparison with the control). Moreover, comparing the protein levels between 1st and 3rd days of SNAP treatment, all proteins (except Stat5 and PECAM-1) were downregulated. These data demonstrate the dynamic cooperation of multiple signaling pathways in the promotion of expansion and differentiation of HSCs under $NO^{\bullet}$ stimulation.

Several reports have shown that proliferation and differentiation in hematopoiesis are linked. For instansce, cycling HSCs show a reduced engraftment potential when exit the G_0 phase [7]. Cytokines such as IL-3, GM-CSF, G-CSF, and M-CSF promote proliferation and differentiation in vitro without reduce the HSC pool [21, 40]. Another factor that seems to be related to hematopoietic cell differentiation is ROS generation. The endosteal niche where most of the HSCs remains quiescent, display low levels of ROS, whereas closer to vascular niche, where HSCs possess great proliferation and differentiation activity, ROS levels are higher [47]. Also, it is in the vascular niche that $NO^{\bullet}$ is physiologically produced by endothelial cells [18, 19, 48]. In addition, cytokine-induced ROS generation has been implicated in G_1 to S progression, which involves the Jak2 and Stat5, as well as the PI3K/Akt and Ras/Mek/ERK signaling pathways [49]. In this study, we observed

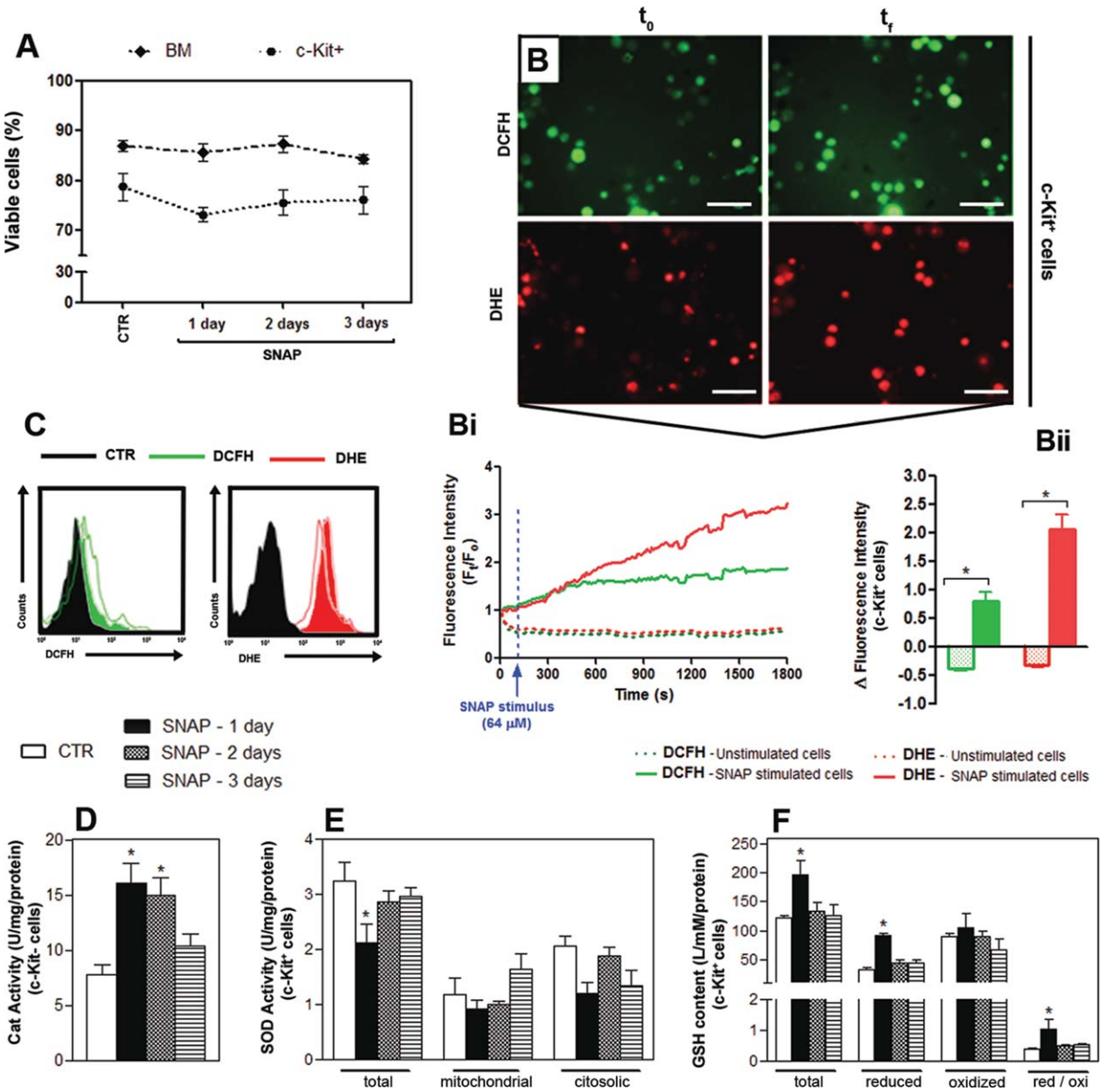

Figure 6. The effect of NO• on hematopoietic cell fate also involves the modulation of cell redox status. **(A, C–F):** Mice were intraperitoneally treated with 0.1 mg/kg of S-nitroso-*N*-acetyl-D,L-penicillamine (SNAP) or **(B)** directly stimulated with 64 μM of SNAP on a plate. **(A):** Cell survival curve of total bone marrow and c-Kit$^+$ cells labeled with annexin-V and 7-aminoactinomycin D (7-AAD), $n = 6$. **(B, C):** Hematopoietic cells were labeled with 5 μM of CM-H_2DCFH-DA and 1 μM of dihydroetidium (DHE) to measure reactive oxygen species (ROS) (mainly H_2O_2) and $O_2^{\bullet -}$, respectively. **(B):** Representative images of ROS generation in SNAP stimulated cells detected in real-time during 30 minutes through fluorescence microscopy (Leica) using a 63× oil objective lens (numerical aperture: 1.47). Scale bar = 40 μm, $n = 4$. **(B-i):** Graph of the fluorescence intensity versus time. **(B-ii):** Δ of fluorescence intensity of unstimulated cells versus SNAP stimulated cells. **(C):** Fluorescence intensity histograms of DHE (red) and DCFH (green) of the control (unfilled) and SNAP-3-day-treated group (filled). Unlabeled cells are shown in the black-filled histogram, $n = 4$. **(D, E)** Spectrophotometric evaluation of catalase and superoxide dismutase. **(F):** Glutathione content was evaluated by high-performance liquid chromatography, $n = 6$. Data normalization was based on total protein content measured by the Bradford method. Data are expressed as the mean ± SEM of independent experiments. *, $p < .05$ analysis of variance test. Abbreviations: BM, bone marrow; CTR, control; DCFH, dichlorofluorescin; DHE, dihydroetidium; GSH, glutathione; SNAP, S-nitroso-*N*-acetyl-D,L-penicillamine; SOD, superoxide dismutase.

that during the HSCs proliferative response, there was an increase in ROS generation and a concomitant modulation of antioxidant enzymes, which might have cooperated in the achievement of a redox steady-state during HSCs differentiation. However, NO• by itself is capable of negatively or positively modulating the hematopoietic system, depending on its mode of action [34, 38, 50]. The importance of a greater understanding on how NO• and other molecules regulate hematopoiesis relies on the fact that this knowledge may give rise to new therapeutic strategies for hematological disorders where the enhancement of proliferation and/or the differentiation of HSCs are desirable, for example, in cases of medullar aplasia, immunosuppression, or previously to bone marrow ablation.

 ©AlphaMed Press 2014

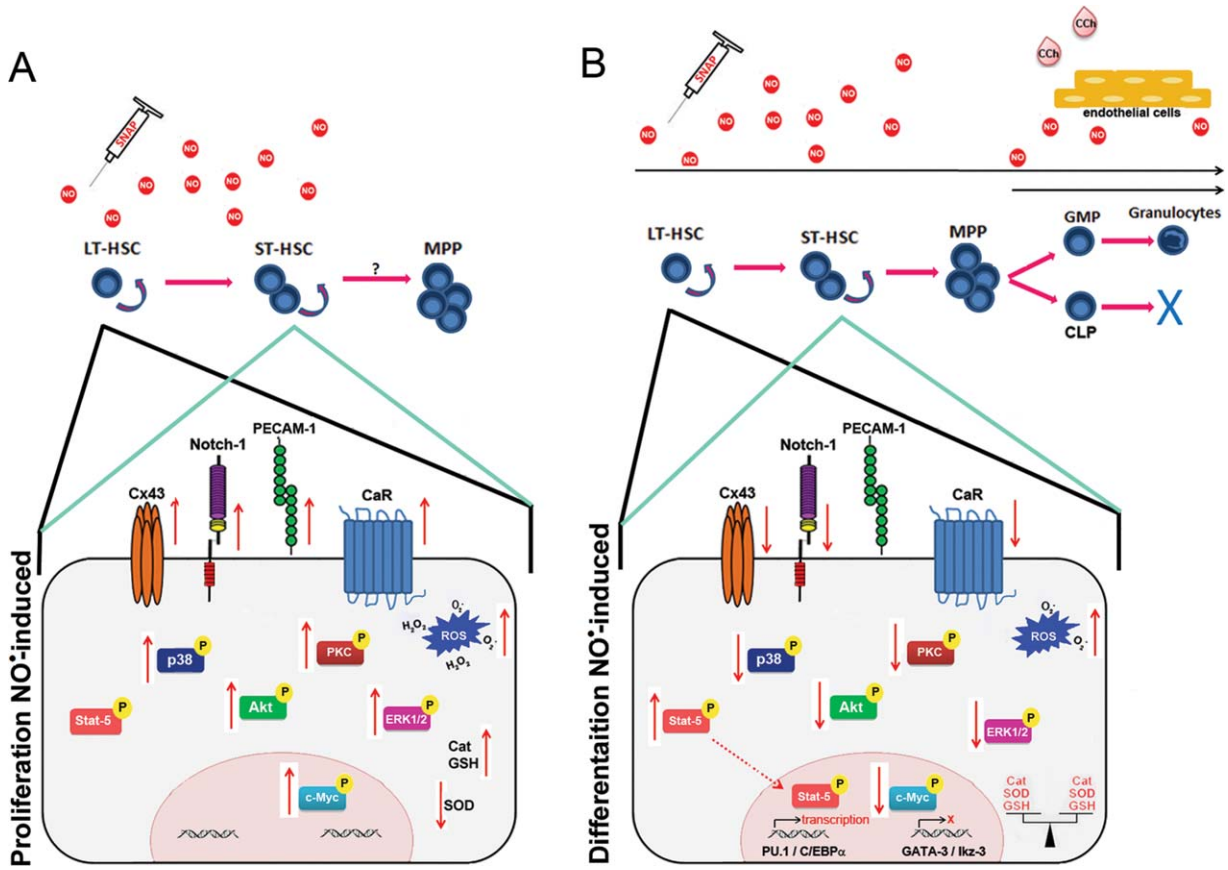

Figure 7. Schematic representation of the effects of NO• on hematopoeisis. **(A):** S-nitroso-*N*-acetyl-D,L-penicillamine (SNAP) treatment induces the proliferation of hematopoietic stem cells (HSCs), which generates ST-HSCs and hematopoietic progenitors. The phosphorylation and expression of important proteins that regulate hematopoiesis are upregulated (↑). Increased reactive oxygen species (ROS) levels are also accompanied by antioxidant regulation, involving the increase in catalase activity and glutathione levels and the reduction in superoxide dismutase (SOD) activity. **(B):** SNAP treatment for 3 days in vivo, as well as NO• generated from endothelial cells that were stimulated by carbachol (CCh) in vitro induces the commitment of HSCs and progenitor cells into granulocyte/monocyte progenitor, leading to terminal differentiation into the myeloid lineage, which is transcriptionally regulated on the overexpression of myeloid proteins (*PU.1* and *C/EBPα*) and the downregulation of lymphoid genes (*GATA-3* and *Ikz-3*). In addition, downregulation (↓) of Akt, ERK1/2, p38, PKC, c-Myc, Notch-1, CaR, and Cx43 proteins occurs, but p-Stat5 is phosphorylated (↑) and PECAM-1 expression remains unchanged in relation to its levels on the 1st day of treatment during the HSCs proliferative response. ROS and antioxidant molecules level returned to baseline conditions (similar to control), whereas $O_2^{\bullet -}$ levels remained elevated. In summary, our data demonstrate NO• ability to trigger the HSCs output from quiescence to active cycling state followed by their differentiation, and also indicates the signaling pathways modulated in these processes. Abbreviations: CLP, common lymphoid progenitor; GMP, granulocyte/monocyte progenitor; LT-HSC, long-term hematopoietic stem cells; MPP, multipotent progenitor; ROS, reactive oxygen species; SOD, superoxide dismutase; ST-HSC, short-term hematopoietic stem cells.

Summary

As shown in Figure 7, it was observed that the exogenous NO• donated by SNAP results in HSCs proliferation in vivo, through the increasing of ST-HSCs and hematopoietic progenitor cells. In addition, NO• produced by endothelial cells and also by SNAP, induces the commitment and differentiation of HSCs to the myeloid progeny giving rise to mature granulocytes, which was characterized by the up and downregulation of PU.1, C/EBPα, GATA-3, and Ikz-3 genes, respectively, which also at the protein level involved Stat5 activation and the downregulation of Notch-1, Cx43, CaR, ERK1/2, Akt, p38, PKC and c-Myc in relation to their activation/expression pattern observed during the proliferative response. Also, the modulation of the intracelular redox system in elevated ROS circumstances was distinctly during proliferation and differentiation of HSCs, which suggests the role of the intracellular redox status in the transition of HSCs responses upon NO• stimuli. The mechanisms through which NO• exerts its roles determining whether the NO•-dependent effects occurs by the classical activation of cyclic guanylate monophosphate or by protein modifications such as S-nitrosylation or tyrosine nitration remain to be investigated.

Acknowledgments

A.N-P. thanks Margaret Gori for technical assistance. This work was supported by INFAR/UNIFESP Confocal and Flow Cytometry Facility, "Coordenação de Aperfeiçoamento de Pessoal de Nível Superior (CAPES)," "Conselho nacional de desenvolvimento científico e Tecnológico (CNPq)," and "Fundação de Amparo à Pesquisa do Estado de São Paulo (FAPESP)." A.N-P. was supported by a Ph.D. fellowship from FAPESP.

Author Contributions

A.N-P.: conception and design, collection and assembly of the data, data analysis and interpretation, and manuscript writing; C.C.D.: collection of the data; P.C.A.: assembly of the data; L.L., M.V.B., and C.C.B, collection and assembly of the data; H.R.C.S., V.D., and E.M.S.H.: provision of study material; E.J.P.-G. and A.T.F.: conception and design, data interpretation, and manuscript writing.

Disclosure of Potential Conflicts of Interest

The authors indicate no potential conflicts of interest.

References

1 Ghaffari S. Oxidative stress in the regulation of normal and neoplastic hematopoiesis. Antioxidant Redox Signal 2008;10:1923–1940.

2 Wang K, Zhang T, Dong Q et al. Redox homeostasis: The linchpin in stem cell self-renewal and differentiation. Cell Death Dis 2013;4:e537.

3 Pfeiffer S, Mayer, B., Hemms, B. Nitric oxide: Chemical puzzles posed by a biological messenger. Angew Chem Int Ed 1999;38: 1714–1731.

4 Miller MR, Megson IL. Recent developments in nitric oxide donor drugs. Br J Pharmacol 2007;151:305–321.

5 Feng X, Sun T, Bei Y et al. S-nitrosylation of ERK inhibits ERK phosphorylation and induces apoptosis. Sci Rep 2013;3:1814.

6 Huerta S, Chilka S, Bonavida B. Nitric oxide donors: Novel cancer therapeutics (review). Int J Oncol 2008;33:909–927.

7 Passegue E, Wagers AJ, Giuriato S et al. Global analysis of proliferation and cell cycle gene expression in the regulation of hematopoietic stem and progenitor cell fates. J Exp Med 2005;202:1599–1611.

8 Lo Celso C, Scadden DT. The haematopoietic stem cell niche at a glance. J Cell Sci 2011;124:3529–3535.

9 Kunisaki Y, Bruns I, Scheiermann C et al. Arteriolar niches maintain haematopoietic stem cell quiescence. Nature 2013;502:637–643.

10 Bianco P. Bone and the hematopoietic niche: A tale of two stem cells. Blood 2011; 117:5281–5288.

11 Wilson A, Trumpp A. Bone-marrow haematopoietic-stem-cell niches. Nat Rev Immunol 2006;6:93–106.

12 Kopp HG, Avecilla ST, Hooper AT et al. The bone marrow vascular niche: Home of HSC differentiation and mobilization. Physiol 2005;20:349–356.

13 Yin T, Li L. The stem cell niches in bone. J Clin Invest 2006;116:1195–1201.

14 Zhu J, Emerson SG. Hematopoietic cytokines, transcription factors and lineage commitment. Oncogene 2002;21:3295–3313.

15 Ito K, Hirao A, Arai F et al. Reactive oxygen species act through p38 MAPK to limit the lifespan of hematopoietic stem cells. Nat Med 2006;12:446–451.

16 Nogueira-Pedro A, Barbosa CM, Segreto HR et al. alpha-Tocopherol induces hematopoietic stem/progenitor cell expansion and ERK1/2-mediated differentiation. J Leuk Biol 2011;90:1111–1117.

17 Paredes-Gamero EJ, Nogueira-Pedro A, Miranda A et al. Hematopoietic modulators as potential agents for the treatment of leukemia. Front Biosci 2013;5:130–140.

18 Forstermann U, Boissel JP, Kleinert H. Expressional control of the 'constitutive' isoforms of nitric oxide synthase (NOS I and NOS III). FASEB J 1998;12:773–790.

19 Furchgott RF, Zawadzki JV. The obligatory role of endothelial cells in the relaxation of arterial smooth muscle by acetylcholine. Nature 1980;288:373–376.

20 Miyashita T, Takeishi Y, Takahashi H et al. Comparison of nitric oxide production in response to carbachol between macrovascular and microvascular cardiac endothelial cells. Circ J 2002;66:511–515.

21 Barbosa CM, Leon CM, Nogueira-Pedro A et al. Differentiation of hematopoietic stem cell and myeloid populations by ATP is modulated by cytokines. Cell Death Dis 2011; 2:e165.

22 Rothaeusler K, Baumgarth N. Evaluation of intranuclear BrdU detection procedures for use in multicolor flow cytometry. Cytometr A: J Int Soc Anal Cytol 2006;69:249–259.

23 De Ciantis PD, Yashpal K, Henry J et al. Characterization of a rat model of metastatic prostate cancer bone pain. J Pain Res 2010;3: 213–221.

24 Duran-Struuck R, Dysko RC. Principles of bone marrow transplantation (BMT): Providing optimal veterinary and husbandry care to irradiated mice in BMT studies. J Am Assoc Lab Animal Sci 2009;48:11–22.

25 Panoskaltsis-Mortari A, Taylor PA, Rubin JS et al. Keratinocyte growth factor facilitates alloengraftment and ameliorates graft-versus-host disease in mice by a mechanism independent of repair of conditioning-induced tissue injury. Blood 2000;96:4350–4356.

26 Adamo AM, Llesuy SF, Pasquini JM et al. Brain chemiluminescence and oxidative stress in hyperthyroid rats. Biochem J 1989;263: 273–277.

27 Ewing JF, Janero DR. Microplate superoxide dismutase assay employing a nonenzymatic superoxide generator. Anal Biochem 1995;232:243–248.

28 Scholzen T, Gerdes J. The Ki-67 protein: From the known and the unknown. J Cell Physiol 2000;182:311–322.

29 Geest CR, Coffer PJ. MAPK signaling pathways in the regulation of hematopoiesis. J Leuk Biol 2009;86:237–250.

30 Smithgall TE. Signal transduction pathways regulating hematopoietic differentiation. Pharmacol Rev 1998;50:1–19.

31 Xu Z, Ji X, Boysen PG. Exogenous nitric oxide generates ROS and induces cardioprotection: Involvement of PKG, mitochondrial KATP channels, and ERK. Am J Physiol Heart Circ Physiol 2004;286:H1433–1440.

32 Gomes A, Fernandes E, Lima JL. Fluorescence probes used for detection of reactive oxygen species. J Biochem Biophys Meth 2005;65:45–80.

33 Napoli C, Paolisso G, Casamassimi A et al. Effects of nitric oxide on cell proliferation: Novel insights. J Am Coll Cardiol 2013; 62:89–95.

34 Michurina T, Krasnov P, Balazs A et al. Nitric oxide is a regulator of hematopoietic stem cell activity. Mol Ther 2004;10:241–248.

35 North TE, Goessling W, Peeters M et al. Hematopoietic stem cell development is dependent on blood flow. Cell 2009;137:736–748.

36 Tiribuzi R, Crispoltoni L, Tartacca F et al. Nitric oxide depletion alters hematopoietic stem cell commitment toward immunogenic dendritic cells. Biochim Biophys Acta 2013; 1830:2830–2838.

37 Krumsiek J, Marr C, Schroeder T et al. Hierarchical differentiation of myeloid progenitors is encoded in the transcription factor network. Plos One 2011;6:e22649.

38 Villalobo A. Enhanced Cell Proliferation Induced by Nitric Oxide. Dyn Cell Biol 2007; 1:60–64.

39 Gharibi B, Ghuman MS, Hughes FJ. Akt- and Erk-mediated regulation of proliferation and differentiation during PDGFRbeta-induced MSC self-renewal. J Cell Mol Med 2012;16:2789–2801.

40 Leon CM, Barbosa CM, Justo GZ et al. Requirement for PLCgamma2 in IL-3 and GM-CSF-stimulated MEK/ERK phosphorylation in murine and human hematopoietic stem/progenitor cells. J Cell Physiol 2011;226:1780–1792.

41 Wilson A, Murphy MJ, Oskarsson T et al. c-Myc controls the balance between hematopoietic stem cell self-renewal and differentiation. Genes Dev 2004;18:2747–2763.

42 Adams GB, Chabner KT, Alley IR et al. Stem cell engraftment at the endosteal niche is specified by the calcium-sensing receptor. Nature 2006;439:599–603.

43 Mendez-Ferrer S, Michurina TV, Ferraro F et al. Mesenchymal and haematopoietic stem cells form a unique bone marrow niche. Nature 2010;466:829–834.

44 Ishikawa ETG-N, D.; Ghiaur, G.; Dunn, S.K.; Ficker, A.M.; Murali, N.; Madhu, M.; Gutstein, D.E.; Fishman, G.I.; Barrio, L.C.; Cancelas, J.A. Connexin-43 prevents hematopoietic stem cell senescence through transfer of reactive oxygen species to bone marrow stromal cells. PNAS 2012;109:9071–9076.

45 Paredes-Gamero EJ, Leon CM, Borojevic R et al. Changes in intracellular Ca2+ levels induced by cytokines and P2 agonists differentially modulate proliferation or commitment with macrophage differentiation in murine hematopoietic cells. J Biol Chem 2008;283:31909–31919.

46 Warr MR, Pietras EM, Passegue E. Mechanisms controlling hematopoietic stem cell functions during normal hematopoiesis

 ©AlphaMed Press 2014

and hematological malignancies. Biol Med 2011;3:681–701.

47 Jang YY, Sharkis SJ. A low level of reactive oxygen species selects for primitive hematopoietic stem cells that may reside in the low-oxygenic niche. Blood 2007;110: 3056–3063.

48 Guerrouahen BS, Al-Hijji I, Tabrizi AR. Osteoblastic and vascular endothelial niches, their control on normal hematopoietic stem cells, and their consequences on the development of leukemia. Stem Cells Int 2011;2011:375857.

49 Iiyama M, Kakihana K, Kurosu T et al. Reactive oxygen species generated by hematopoietic cytokines play roles in activation of receptor-mediated signaling and in cell cycle progression. Cell Signal 2006; 18:174–182.

50 Villalobo A. Nitric oxide and cell proliferation. FEBS J 2006;273:2329–2344.

See www.StemCells.com for supporting information available online.